
Time Delays for Anisotropic Diffuse Continuum Emission - a Case Study for NGC 5548

Daniel (unclellama@gmail.com), Mike, Otho, Kirk

1 INTRODUCTION

2 PRESSURE-LAW BROAD-LINE REGION MODELS

We denote models for which the pressure P depends on the radius r as

$$P(r) \propto r^{-s}.$$

as pressure-law BLR models. In this work we examine the extreme cases, $s = 0$ and $s = 2$. Evidently, $s = 0$ corresponds to a constant pressure as a function of radius; we show below that $s = 2$ corresponds to a constant ionization parameter. A power-law pressure distribution leads to the following relations (e.g., Rees+1989, Goad+1993). Assuming that the clouds have a constant temperature, the cloud hydrogen density n_{H} is proportional to the pressure:

$$n_{\text{H}}(r) \propto r^{-s}$$

The ionization parameter U at ionizing photon-counting flux $Q(\text{H})$ is defined as:

$$U = Q(\text{H}) / (4\pi r^2 c n_{\text{H}})$$

Thus, $s = 2$ corresponds to a constant ionization parameter.

$$U(r) \propto r^{s-2}$$

The surface area per cloud, A_c , is proportional to R_c^2 , where R_c denotes the radius of a cloud. In general, R_c depends on the pressure P , and is therefore constant for $s = 0$. If we demand that the mass of each cloud is conserved as the clouds move radially (i.e., clouds do not break

up or coalesce within our region of interest), mass conservation implies that $R_c^3 n_H$ is constant. Thus, we obtain the relation

$$A_c(r) \propto R_c^2(r) \propto r^{2s/3}.$$

The column density of each cloud, N_{col} , depends on the gas density and cloud radius:

$$N_{\text{col}}(r) \propto R_c N_H$$

According to the above, both the column density N_{col} and the cloud density n_H are constant for $s = 0$. Therefore, for the constant-pressure case, we work with constant- n_H slices through *Cloudy* grids generated at a given N_{col} .

3 METHOD: FROM *Cloudy* GRIDS TO BLR MODELS

3.1 RESPONSIVITY-WEIGHTED LAGS

3.2 ANISOTROPIC EMISSION

4 RESULTS

4.1 STEADY-STATE MODELS

4.2 MEAN LAGS FOR EMISSION LINES

4.3 THE DIFFUSE CONTINUUM

4.3.1 THE REVERBERATION SIGNATURE OF THE DIFFUSE BALMER CONTINUUM

4.4 GETTING THE NORMALIZATION FOR $A_c(r)n_c(r)$

The total luminosity for a BLR line is given by the integral

$$L = 4\pi \int_{r_{\text{in}}}^{r_{\text{out}}} \epsilon(r) A_c(r) n_c(r) r^2 dr$$

Here, ϵ denotes the line emissivity per cm^2 of cloud surface, and $n_c(r)$ is the number density of clouds. Assuming a power-law distribution $n_c \propto r^{-p}$, and virial motion of the clouds ($v(r) \propto r^{-1/2}$), mass conservation implies the following relation for the differential covering factor:

$$dC(r) \propto A_c(r) n_c(r) dr \propto r^{2s/3-3/2} dr$$

This relation allows us to determine a normalization constant for the total line-emitting surface of the clouds (the volume integral of $A_c(r)n_c(r)$), for a given total covering factor of the central source (the solid angle Ω covered by a single cloud ‘as seen from the source’ goes as $d\Omega = dA_c/r^2$). The normalization factor can be found analytically for a given s , or determined numerically - after some debugging, both approaches agree! The luminosity integral becomes:

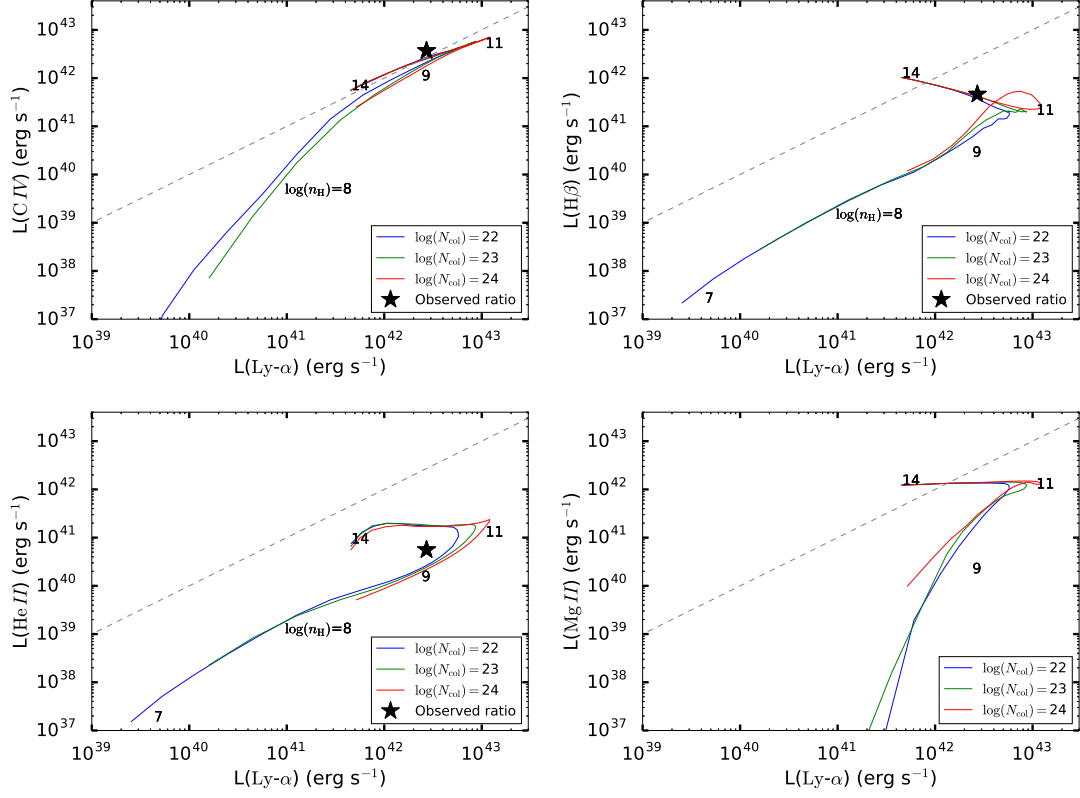


Figure 4.1: Line luminosity ratios for CIV, H β , He II 4686Å and Mg II, relative to Ly α , for the $s = 0$ (constant pressure) steady-state model. The black stars represent the observed, dereddened line ratios, after subtraction of a narrow-line component (CITE DeRosa+17 for UV, Pei+17 for opt., K+G2000 for UV line decomposition, Peteson+199 for Hbeta decomposition.). These values of L_{line} assume that the BLR covers 4π str of the continuum source (see discussion in 4.1).

$$L = 4\pi k \int_{r_{in}}^{r_{out}} \epsilon(r) r^{2s/3+1/2} dr$$

where k is the scaling constant found by integrating over dC .

4.5 GETTING THE INTEGRATED LINE LUMINOSITIES

We have a grid of *Cloudy* models for each emission line, providing the emissivity ϵ , as a function of n_H , N_{col} , and the ionizing flux $\Phi(H)$. For a given source luminosity and SED shape, the Φ axis in these grids can be converted into a radial axis, allowing the evaluation of the integral L . The resulting line luminosities thus depend on n_H , N_{col} , the ionizing continuum SED, the inner and outer BLR radii, and the total covering fraction of the BLR. The dependence of L on r_{in} is strong for $s = 0$, in the sense that smaller inner radii lead to smaller integrated luminosities - this is due to the model distributing most of the clouds close to the inner radius, where they become overionized if the inner radius is small.

To start with we assume total coverage of the continuum source, so as to obtain an upper limit on the line luminosities attainable. We assume an inner BLR radius of 1 lightday (as suggested by RM monitoring), and an outer radius of 140 lightdays (as set by the dust sublimation radius for our adopted source luminosity).

5 LINE LUMINOSITIES AND EFFECTIVE RADII AS A FUNCTION OF n_H

5.1 MATCHING THE OBSERVED LINE LUMINOSITIES

Figure ??, top left panel, shows the line luminosities produced for the $\text{Ly}\alpha$, c IV, and $\text{H}\beta$ emission lines, as a function of n_H , for $N_{col} = 10^{23} \text{ cm}^{-2}$. (We find that, for intermediate values of n_H , the resulting luminosities are not strongly sensitive to N_{col} over the range $22 \leq \log(N_c) \leq 24$.)

Ideally we want these luminosities to be larger than the observed, dereddened line luminosities, as this will allow us to assume a smaller covering fraction - our model does not take BLR self-shadowing into account, so becomes unreliable at high covering fractions. At $\log n_H \sim 11$, our $s = 0$ model can exceed the observed broad-line luminosities for $\text{Ly}\alpha$ and c IV, but has trouble reproducing the observed $\text{H}\beta$ flux.

5.2 EFFECTIVE RADII OF THE LINE-EMITTING REGIONS

Figure ??, bottom right panel, shows the effective radii in light-days, using luminosity-weighting. I.e., the radius is weighted towards the regions that produce more of the total luminosity. For $n_H < 10$, the luminosity-weighted radii of the three lines are very similar - in a constant-pressure BLR with clouds below this density, the three lines would appear to be produced at

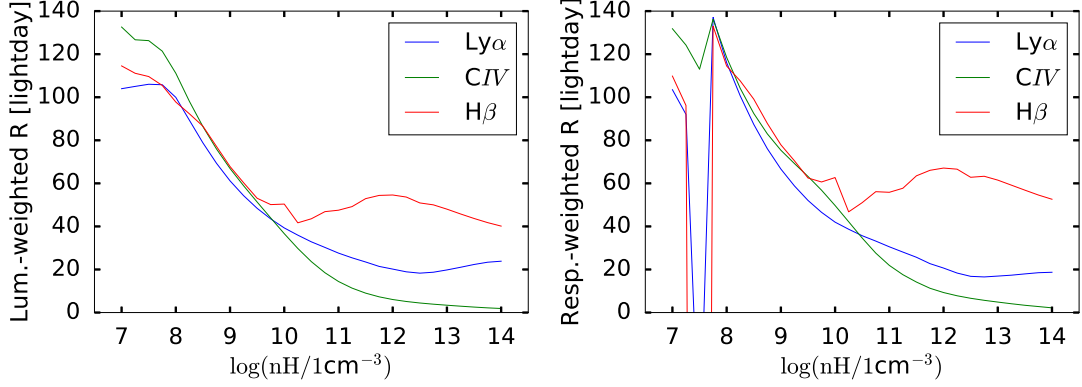


Figure 5.1: Effective BLR radii as a function of n_H , using luminosity-weighting (left panel) and responsivity-weighting (right panel).

the same radii.

In Figure 5.1 we compare the luminosity-weighted radii with responsivity-weighted radii. The responsivities $\eta(r)$ are defined as $\eta = d \log(\epsilon(r)) / d \log(\Phi(r))$. Thus, $\eta = 1$ implies that the equivalent width of a line is constant for a small change in the ionizing flux level. The responsivity-weighted radii are more relevant to RM campaigns, as they give the radius at which we will preferentially see emission line response to continuum variations. For these emission lines, we tend to see larger emissivity-weighted radii compared to luminosity-weighted, i.e., the gas at larger radii responds more strongly to the continuum flux.

Note: at very low densities $\log n_H < 8$, the responsivities are negative for much of the inner region of the BLR - and, as the BLR is sparsely sampled in Φ here, there are likely numerical issues with my code, giving strongly negative responsivity-weighted radii here - need to look into this more!

6 DIFFUSE CONTINUUM FOR $N_H = 11$

The ‘diffuse continuum’ is the continuum emission produced by the BLR clods themselves. As we found that models with $\log n_H \sim 11$ produce enough luminosity to roughly match or exceed the observed emission line levels, we now examine the diffuse continuum produced for the pressure law BLR with constant density $\log n_H = 11$. The *Cloudy* grids provided include the diffuse continuum emissivity in several wavelength bands, again as a function of n_H , $\Phi(H)$, and N_{col} ; we integrate the total luminosity of each of these bands in the same way as for the emission lines, providing a spectrum of νL_ν as a function of wavelength for the diffuse continuum (Figure 6.1, top left). Note the strong Balmer continuum feature at wavelengths below the Balmer break ~ 3646 Ang.

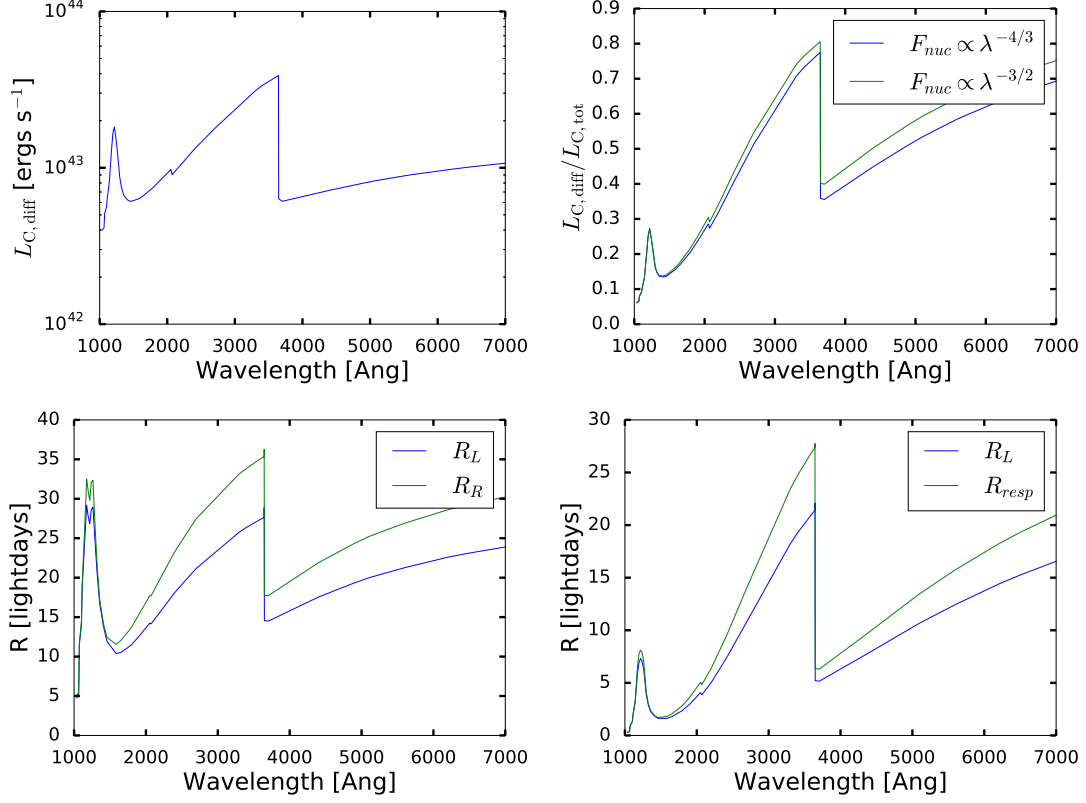


Figure 6.1: Top left: diffuse BLR continuum νF_{nu} as a function of wavelength. Top right: Ratio of diffuse continuum to total (nuclear + diffuse) continuum luminosity, as a function of wavelength. Bottom left: Effective radii for the diffuse continuum. Bottom right: effective radii for the total + diffuse continua, assuming that the nuclear continuum is a point source at all wavelengths.

Assuming a power-law form for the nuclear continuum, extrapolated from the continuum luminosity at 1215 Ang, we calculate the ratio of diffuse continuum to total (nuclear + diffuse) as a function of wavelength. The diffuse continuum exceeds the nuclear continuum emission near the Balmer break (Figure 6.1, top right). As for the emission lines, we can find the luminosity-weighted and emissivity-weighted radii for the diffuse continuum (bottom left panel), and the effect of diluting the diffuse continuum emission with the appropriate fraction of nuclear-continuum light (assuming the latter is a point-source). It is interesting that these models predict elevated continuum delays near the Balmer break, relative to the $R \propto \lambda^{-4/3}$ dependence suggested for emission from the surface of an accretion disk.